Dynamics of Trion Formation in $In_xGa_{1-x}As$ Quantum Wells

M. T. Portella-Oberli,[1] J. Berney,[1,2] L. Kappei,[1] F. Morier-Genoud,[1] J. Szczytko,[1,3] and B. Deveaud-Plédran[1]

[1]*Institut de Photonique et Electronique Quantiques, Ecole Polytechnique Fédérale de Lausanne (EPFL), CH1015 Lausanne, Switzerland*

[2]*Attolight Sàrl, CH1024 Ecublens, Switzerland*

[3]*Institute of Experimental Physics, Warsaw University, Hoża 69, 00-681 Warsaw, Poland*

(Received 24 January 2008; revised manuscript received 23 January 2009; published 3 March 2009)

We show a double path mechanism for the formation of charged excitons (trions); they are formed through bi- and trimolecular processes. This directly implies that both negatively and positively charged excitons coexist in a quantum well, even in the absence of excess carriers. The model is substantiated by time-resolved photoluminescence experiments performed on a very high quality $In_xGa_{1-x}As$ quantum well sample, in which the photoluminescence contributions at the energy of the trion and exciton and at the band edge can be clearly separated and traced over a broad range of times and densities. The unresolved discrepancy between the theoretical and experimental radiative decay time of the exciton in a doped semiconductor quantum well is explained by the same model.

DOI: 10.1103/PhysRevLett.102.096402 PACS numbers: 71.35.Cc, 71.35.Ee, 73.21.Fg, 78.47.−p

Positively and negatively charged excitons (X^+ and X^- trions) [1,2] are usually compared to their atomic counterpart ions of helium He^+ and hydrogen H^-, respectively. In astronomy, the dynamics of the formation of these atomic ions is of great importance [3]; indeed, H^- is the primary source of the continuum opacity in most stellar photospheres and contributes to the production of hydrogen and other elements in various parts of the Universe. Additionally, the abundance of free electrons in the solar atmosphere is indirectly measured in terms of H^- concentration. In semiconductor quantum wells (QWs), trions show a number of properties very similar to excitons [4], such as strong coupling in microcavities [5], absorption bleaching [6,7], transport [8] and diffusion [9] properties, and radiative recombination efficiency [10,11], and thus have attracted considerable interest. Moreover, trions promise to play a key role in future applications, notably in quantum-information science [12] and in the future development of all-spin-based scalable quantum computers [13,14]. They are correlated with excitons and the free carrier plasma and offer the possibility to test a model of formation of three-particle complexes.

The formation process of neutral excitons (X) in QWs has been extensively investigated over the past two decades [15,16] and recently shown to be strongly density- and temperature-dependent [17]. This is a bimolecular process, in which an electron (e) and a hole (h) are bound by Coulomb interaction with the emission of the appropriate phonon. Conversely, the formation process of trions has been much less studied. It is largely believed that trions can be formed only if a population of excess carriers is trapped in the well, producing exclusively trions with the same charge. Consequently, existing models discriminate the formation channel yielding trions of opposite charge. Current models for trion formation [18,19] surmise that trions are exclusively formed through a bimolecular process, i.e., the coalescence of an exciton and a charged free carrier. While this is conceivable at low densities, nothing attests that genuine formation of the trion from an unbound electron-hole plasma (trimolecular formation) is negligible at higher densities.

In this Letter, we address this fundamental problem and propose a formation model that fully implements bi- and trimolecular channels for both negatively and positively charged excitons. We investigate the trion binding dynamics by following separately the evolution of the exciton, trion, and plasma luminescence, which is possible by using a time-resolved photoluminescence setup of increased sensitivity. We demonstrate the complexity of many-body effects in the trion formation and show that all of the assumptions made in our model are necessary to describe adequately experiments over a broad range of excess carrier densities. Moreover, we show that the higher the carrier concentration, the more important the trimolecular process. Theoretical calculations corroborate these results and evidence that momentum conservation of carriers is important in the trion formation process.

The sample used for this study is a single $In_xGa_{1-x}As$ 80 Å QW, with an indium content of about $x = 5\%$ grown by molecular-beam epitaxy. It is kept at 5 K. The cw photoluminescence spectra are recorded with a CCD camera and time-resolved spectra with a streak camera in photon-counting mode. The temporal resolution of the whole setup is limited to about 10–20 ps, due to the dispersion of the grating, allowing a 0.1 meV spectral resolution. More details about the characterization of the sample and the experimental setup can be found in [17,20]. With proper excitation energy $\hbar\omega$, we control the electron density accumulated in the well, as shown in Fig. 1, where we compare the cw luminescence of the sample collected for $\hbar\omega = 1.5072$ eV and $\hbar\omega = 1.5174$ eV. Since the trion luminescence is affected by the concentration of charged

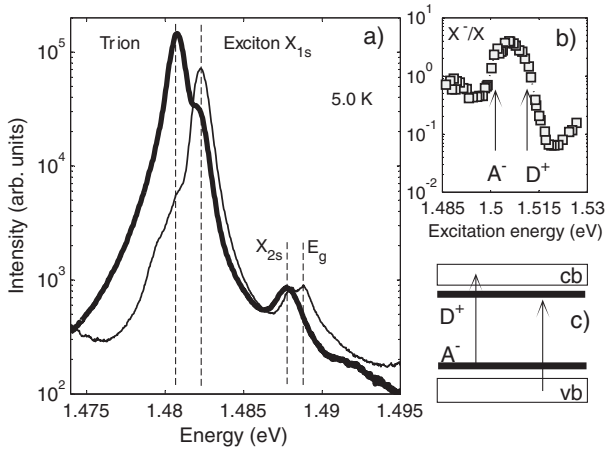

FIG. 1. (a) cw luminescence collected for two different excitation energies: $\hbar\omega = 1.5072$ eV (thick line) and $\hbar\omega = 1.5174$ eV (thin line). The structures at 1.4807 eV, 1.4823 (1.4882 eV), and $E_g = 1.4888$ eV correspond, respectively, to the trion, heavy-hole exciton $1s$ ($2s$), and plasma transitions (all denoted by vertical dashed lines). (b) The intensity ratio of the trion to exciton transitions as a function of the excitation energy. (c) Schematic diagram of the electronic transitions from the ionized acceptors A^- to the conduction band cb and from the valence band vb to the ionized donors D^+.

carriers in the well, the relative X^--to-X intensity changes with the excitation energy [Fig. 1(b)]. The carriers trapped into the QW come from the impurities unintentionally introduced in the GaAs barriers during the growth process (carbon and silicon). Electrons appear when the excitation energy exceeds the energy between ionized acceptors and the conduction band. The electrons photoexcited in the conduction band may then be trapped into the QW. With increasing excitation energy, one can transfer electrons from the valence band to ionized donors, thereby increasing the density of holes, which then eliminate electrons [Fig. 1(c)]. The excess carriers trapped in the QW have a tunneling time back to the charge centers in the barriers several orders of magnitude longer than the 12 ns repetition time of the laser used in time-resolved experiments. Therefore, the population of available acceptor states in the barrier is quickly fully depleted even at low photon density and under pulsed excitation. We have carried out the present experiments with an excitation energy of 1.5072 eV to get a large enough trion population in the well. The background electron density is given by the concentration of ionized acceptors in the barrier, which is determined by growth conditions of the sample and is of the order of 10^{10} cm^{-2}.

In order to study the dynamics of the luminescence in different density domains, we performed time-resolved experiments with a variety of absorbed photon densities (10^8–10^{10} cm^{-2}). Then, to obtain the time evolution of the exciton, trion, and plasma populations, for each time delay we spectrally integrate each transition. Because of the low excitation density used in the present experiments, we use the line shapes carefully deduced from the cw experiments. In Fig. 2, we show the time evolution of the exciton, trion, and plasma concentrations obtained from this analysis.

The luminescence dynamics is governed by the temporal evolution of the population of free carriers, excitons, and trions. We first make an inventory of all channels that couple efficiently those populations. Apart from the known exciton bimolecular formation $e + h \leftrightarrow X$, we identify for trions two bimolecular reactions ($X + e \leftrightarrow X^-$ and $X + h \leftrightarrow X^+$) and two trimolecular reactions ($2e + h \leftrightarrow X^-$ and $e + 2h \leftrightarrow X^+$) involving trions. The biexciton and Auger channels are neglected because they are not significant at these densities [17]. The kinetics of these reactions is given in terms of five coupled rate equations:

$$\frac{dn}{dt} = -Bnp - \frac{n}{\tau_{\rm nr}} - F^X - F_2^{X^-} - F_3^{X^-} - F_3^{X^+} + \frac{\mathcal{X}^-}{\tau_{X^-}},$$

$$\frac{dp}{dt} = -Bnp - \frac{p}{\tau_{\rm nr}} - F^X - F_2^{X^+} - F_3^{X^+} - F_3^{X^-} + \frac{\mathcal{X}^+}{\tau_{X^+}},$$

$$\frac{d\mathcal{X}}{dt} = F^X - \frac{\mathcal{X}}{\tau_D} - F_2^{X^-} - F_2^{X^+}, \quad \frac{d\mathcal{X}^-}{dt} = F_2^{X^-} + F_3^{X^-} - \frac{\mathcal{X}^-}{\tau_{X^-}},$$

$$\frac{d\mathcal{X}^+}{dt} = F_2^{X^+} + F_3^{X^+} - \frac{\mathcal{X}^+}{\tau_{X^+}},$$

where the free carrier concentrations n (electrons) and p

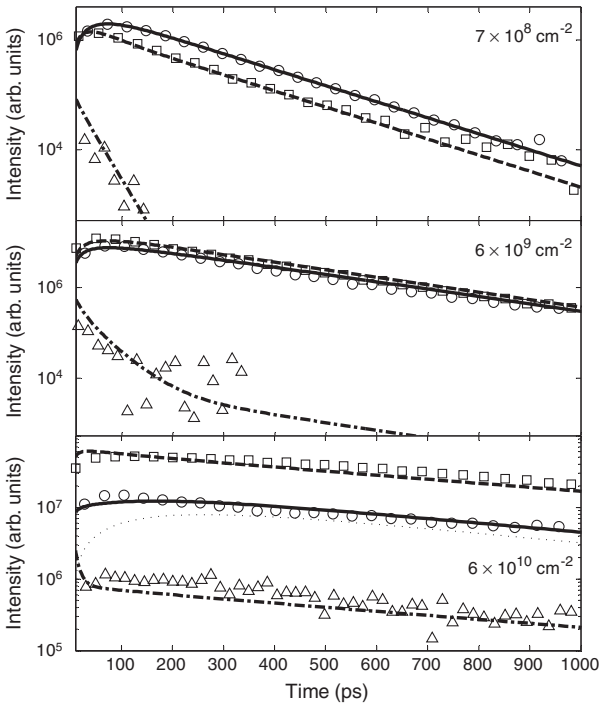

FIG. 2. The intensity of the luminescence of trions (solid line, circles), excitons (dashed line, squares), and plasma (dashed-dotted line, triangles) calculated according to rate equations (lines) compared with experimental data (symbols) for 7×10^8, 6×10^9, and 6×10^{10} cm^{-2} absorbed photon densities. At 6×10^{10} cm^{-2} density, the best fit for trions after artificially enforcing $A_3 = 0$ (dotted line): $\mathcal{N} = 10^{10}$ cm^{-2}.

(holes) decay through—in order of appearance—the radiative and nonradiative recombination rates, the exciton formation rate F^X, and the trion formation rates $F_2^{X^\alpha}$ (bimolecular) and $F_3^{X^\alpha}$ (trimolecular), $\alpha = \{-, +\}$. The term $\mathcal{X}^\alpha/\tau_{X^\alpha}$ corresponds to the carriers recycled after the radiative decay of the trions. The exciton and trion populations $\mathcal{X}$, $\mathcal{X}^-$, and $\mathcal{X}^+$ decay through radiative recombination. Additionally, excitons decay through trion formation. The different formation rates read $F^X = \gamma C n p - \gamma C K_X \mathcal{X}$, $F_2^{X^-} = A_2^- \mathcal{X} n - A_2^- K_2^- \mathcal{X}^-$, $F_3^{X^-} = A_3^- n n p - A_3^- K_3^- \mathcal{X}^-$, $F_2^{X^+} = A_2^+ \mathcal{X} p - A_2^+ K_2^+ \mathcal{X}^+$, and $F_3^{X^+} = A_3^+ n p p - A_3^+ K_3^+ \mathcal{X}^+$, where the equilibrium coefficients K_X, K_2^α, and K_3^α are given by the steady-state solution of the rate equations [17,21,22].

A few simple considerations allow us to reduce significantly the number of free parameters. The equilibrium coefficients can be calculated from a mass action law, exploiting the fact that the trion binding energies for both X^- and X^+ are equal [23]. The values of the bimolecular plasma recombination rate B and bimolecular exciton formation rate γC are known [17]. Because of the high quality of the sample, we have a very long nonradiative decay time τ_{nr} that is negligible. Knowing the number of photons $\mathcal{N}_{h\nu}$ absorbed in our sample, we use the initial parameters $p = \mathcal{N}_{h\nu}$ and $n = \mathcal{N}_{h\nu} + \mathcal{N}$, where the excess electron concentration is estimated from impurity concentration: $\mathcal{N} = 10^{10}$ cm^{-2}. We have introduced the equations of formation for positive trions for the sake of completeness. However, our present measurements are not sensitive to the X^+ population, and we have decided to equate A_2^+ with A_2^- and A_3^+ with A_3^-. Once we have found an expression for the thermalized exciton and trion radiative decay times τ_D and τ_{X^α}, A_2 and A_3 will be the only parameters left.

We assume that excitons, trions, and free carriers are thermalized and share the same temperature T_c, different from the lattice temperature T_l. This is justified because exciton, carrier, and carrier-carrier scatterings are very fast [24–26]. In our time-resolved experiment, we use three electron-hole pair densities 7×10^8, 6×10^9, and 6×10^{10} cm^{-2}. At the highest density, T_c is given by the exponential fit to the high-energy tail of the free carrier luminescence. This temperature is 35 ± 5 K. At lower densities, the rapid plasma relaxation prevents us from measuring T_c that way. Yet, it can be trivially calculated if we depict the accumulated excess carriers trapped in the QW as a cold sea of electrons at T_l, in which the electron-hole pairs injected by the optical pump efficiently thermalize. We get 9 and 16 K. At last, the temperature dependence of the radiative decay rates $\tau_D(T_c)$ and $\tau_{X^\alpha}(T_c)$ is most accurately described by the linear laws $\tau_D(T_c) = 20 \times T_c$ [ps] and $\tau_{X^\alpha} = 78 + 7 \times T_c$ [ps] (with T_c in [K]). Apart from a factor of 1.5 attributed to the Bragg mirrors that enhances the coupling of the excitons and charged excitons to the field and hence diminishes the radiative decay time, the agreement with the expected theoretical behavior is very good [10,11,27].

We present the complete results of our calculations of excitonic, trion, and plasma luminescence intensity dynamics in Fig. 2. The excitonic luminescence intensity given by $\mathcal{X}/\tau_D$ is denoted by a dashed line. The luminescence intensities of X^- and X^+ are summed up ($\mathcal{X}^-/\tau_{X^-} + \mathcal{X}^+/\tau_{X^+}$) and denoted by solid lines. The free carrier luminescence Bnp is denoted by a dashed-dotted line. Even with the necessary simplifications mentioned above, the rate equations provide a very good description of the observed time-resolved luminescence spectra. It is important to keep in mind that there is no adjustment between the different panels of Fig. 2: Our parameters strictly describe the whole range of densities. For instance, for the smallest excitation densities the strongest transition comes from the trions, while for the larger densities the exciton transition dominates. Interestingly, for the lowest excitation density, trion and exciton dynamics are much faster than for the highest, in striking contrast with the exciton dynamics in undoped QWs [17]. We may understand this fast luminescence dynamics in the low density regime: This is mostly the effect of the change of the temperature of carriers (and therefore of trions and excitons). If we impose the same temperature for all excitation densities, τ_D and τ_{X^α} then stay constant over the densities, and we get, as expected, slower dynamics for lower than for higher densities.

We report in Fig. 3 the parameters A_2^α and A_3^α derived from our fit (dots). We also performed a theoretical calculation of the bi- and trimolecular formation dependence on temperature [21] based on the formalism developed by Piermarocchi *et al.* for exciton formation [15]. The results of the calculation are shown on Fig. 3 (lines) after having been multiplied by a factor of 1.5. Experimental and theoretical results have the same temperature dependence, which directly comes from the momentum and energy conservation of carriers. Second, it turns out that both bi- and trimolecular channels are essential to the generation of trions. At high carrier densities, i.e., short times or large densities, the trimolecular process even dominates the bimolecular. This is shown by the thin dotted fit in Fig. 2, calculated after having artificially eliminated the

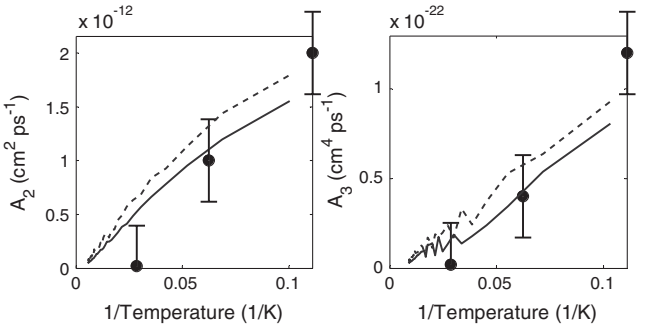

FIG. 3. The bi- and trimolecular trion formation coefficients A_2^α and A_3^α as a function of the inverse carrier temperature. The dots correspond to the formation coefficients obtained from the fit. The solid (dashed) lines shows the value expected from the theory for A^- (A^+).

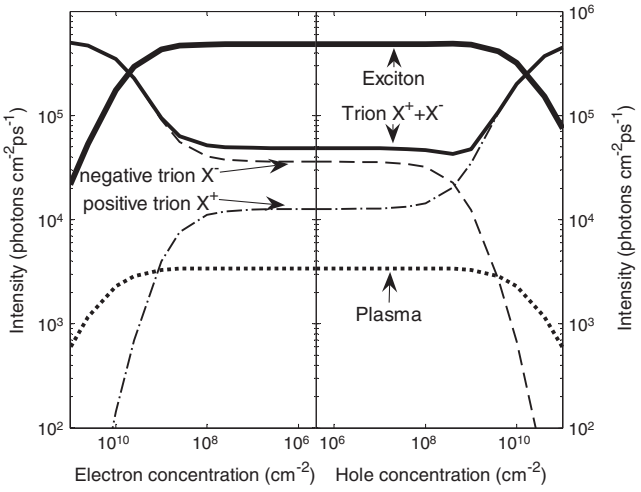

FIG. 4. Exciton, trion (X^- and X^+), and plasma cw-luminescence intensities calculated as a function of the residual electron (left panel) and hole (right panel) concentrations at $T_c = 9.0$ K. A 5×10^5 photons/(cm^2 ps) density was assumed.

A_3 component. Finally, we demonstrate through our calculation that A_2^- and A_3^- are approximately equal to A_2^+ and A_3^+, respectively, which confirms our initial assumption. The trion formation time from a resonantly excited gas of excitons was indeed measured in CdTe QWs for both X^- [28] and X^+ [29], and the formation times turned out to be equivalent. The bimolecular coefficient drawn from those experiments ($A_2 \approx 3 \times 10^{-12}$ cm^2/ps) matches ours.

We demonstrate the robustness of our model by some convincing predictions. In Fig. 4, we apply our rate equations model to the cw luminescence of excitons, trions, and free carriers in an InGaAs QW. In the absence of excess carriers ($n = p$), the trion luminescence is about 20 times weaker than the exciton one, which is in very good agreement with experiments [23]. The difference in intensities of X^- and X^+ cw luminescence shown in Fig. 4 are the consequence of the difference between K_2^α and K_3^α, imposed by the mass difference between positive and negative trions. The critical carrier concentration of about 10^{10} cm^{-2} at which trions start to dominate the luminescence spectrum does correspond to many experiments [30]. What is new, however, is that the crossing of X^- and X^+ intensities, which has been observed experimentally [23], does not occur at zero excess carrier density but is shifted toward some positive carrier density.

Applied to a system of excitons under resonant excitation, our model explains a very puzzling decay time of excitons, which is raised from 20 to 100 ps in the presence of an excess electron gas [31]. Excitons and trions actually come into thermal equilibrium and decay together, which considerably stretches the decay time.

In summary, we have shown that both bi- and trimolecular processes are necessary to describe trion formation. We could quantify both formation rates from the experiment and show that they match the theoretical temperature dependence. We obtained new insight on X^- and X^+ luminescence intensities at low excess carrier densities. The model turned out to also be perfectly applicable to other experiments.

We acknowledge financial support from FNRS within quantum photonics NCCR. We thank D. Y. Oberli and M. Richard for enlightening discussions.

[1] K. Kheng *et al.*, Phys. Rev. Lett. **71**, 1752 (1993).
[2] G. Finkelstein *et al.*, Phys. Rev. Lett. **74**, 976 (1995).
[3] A. M. Frolov *et al.*, J. Chem. Phys. **119**, 3130 (2003).
[4] D. S. Chemla *et al.*, J. Opt. Soc. Am. B **2**, 1155 (1985).
[5] R. Rapaport *et al.*, Phys. Status Solidi **227**, 419 (2001).
[6] M. T. Portella-Oberli *et al.*, Phys. Rev. B **69**, 235311 (2004).
[7] J. Berney *et al.*, Phys. Rev. B **77**, 121301(R) (2008).
[8] D. Sanvitto *et al.*, Science **294**, 837 (2001).
[9] M. T. Portella-Oberli *et al.*, Phys. Rev. B **66**, 155305 (2002).
[10] A. Esser *et al.*, Phys. Rev. B **62**, 8232 (2000).
[11] V. Ciulin *et al.*, Phys. Rev. B **62**, R16 310 (2000).
[12] X. Q. Li *et al.*, Science **301**, 809 (2003).
[13] C. Piermarocchi *et al.*, Phys. Rev. Lett. **89**, 167402 (2002).
[14] E. Pazy *et al.*, Europhys. Lett. **62**, 175 (2003).
[15] C. Piermarocchi *et al.*, Phys. Rev. B **55**, 1333 (1997).
[16] K. Siantidis *et al.*, Phys. Rev. B **65**, 035303 (2001).
[17] J. Szczytko *et al.*, Phys. Rev. Lett. **93**, 137401 (2004).
[18] C. Jeukens *et al.*, Phys. Rev. B **66**, 235318 (2002).
[19] E. Vanelle *et al.*, Phys. Rev. B **62**, 2696 (2000).
[20] J. Szczytko *et al.*, Phys. Status Solidi C **1**, 493 (2004).
[21] J. Berney *et al.*, arXiv:0901.3645.
[22] R. T. Philips *et al.*, Solid State Commun. **98**, 287 (1996).
[23] S. Glasberg *et al.*, Phys. Rev. B **59**, R10 425 (1999).
[24] W. H. Knox, *Optical Studies of Femtosecond Carrier Thermalization in GaAs* (Academic Press, San Diego, 1992), p. 313.
[25] A. Honold *et al.*, Phys. Rev. B **40**, 6442 (1989).
[26] G. Ramon *et al.*, Phys. Rev. B **67**, 045323 (2003).
[27] B. Deveaud *et al.*, Phys. Rev. Lett. **67**, 2355 (1991).
[28] M. T. Portella-Oberli *et al.*, Phys. Status Solidi B **238**, 513 (2003).
[29] P. Plochocka *et al.*, Phys. Rev. Lett. **92**, 177402 (2004).
[30] P. Kossacki, J. Phys. Condens. Matter **15**, R471 (2003).
[31] G. Finkelstein *et al.*, Phys. Rev. B **58**, 12 637 (1998).